

Effect of Surfactant on Flow Boiling Heat Transfer of Ethylene Glycol/Water Mixtures in A Mini-tube

Zhaozan FENG¹, Zan WU^{2,*}, Wei LI¹, Bengt SUNDEN²

* Corresponding author: Tel.: +46 46 2228604; Fax: +46 46 2224717; Email:
zan.wu@energy.lth.se

¹ Department of Energy Engineering, Zhejiang University, Hangzhou, China

² Department of Energy Sciences, Lund University, Lund, Sweden

Abstract In this study, the effect of adding a surfactant (sodium dodecylbenzene sulfonate, SDBS) to ethylene glycol/water mixtures boiling in a vertical mini-tube was studied. Experiments were done using solutions containing 300 ppm by weight of surfactant and the results were compared with those for pure mixture. Local heat transfer coefficient was measured and found to be dependent on the mass quality. Addition of surfactant significantly enhanced the evaporation of saturated liquid, so that the difference between outlet fluid temperature and outlet bubble point temperature of SDBS solutions was much higher than that of ethylene glycol/water mixture. Though the surfactant intensifies the vaporization process, it does not necessarily enhance the heat transfer coefficient. The heat transfer coefficients at two different mass fluxes were compared, and the result could be explained based on the local flow pattern and heat transfer mechanism. After a critical quality, higher quality will deteriorate the heat transfer due to intermittent dryout, therefore adding surfactant to generate more vapor may have a negative effect on the heat transfer of flow boiling in a mini-tube, which is contrast to the experience of enhancing nucleate pool boiling heat transfer with trace surfactant.

Keywords: Nanofluid, Surfactant, Ethylene glycol/water mixture, Flow boiling, Mini-tube

1. Introduction

Nanofluids are engineered colloidal suspensions of nanometer-sized particles in conventional heat transfer fluids such as water, glycol, or their mixtures. Nanometer-sized particles have overcome the challenges of using micrometer and millimeter sized particles with respect to stability, clogging and erosion in the channels. Extensive studies have been conducted on the thermophysical properties and heat transfer characteristics of nanofluids. However, there are apparent inconsistencies in various statements about the enhancement of thermal conductivity and heat transfer coefficient. A possible reason for this puzzle might be the preparation procedure of nanofluids, especially the addition of surfactant such as sodium dodecylbenzene sulfonate (SDBS). Due to the high surface energy of nanoparticles, the colloidal system might become less stable. SDBS could

efficiently improve the stability of nanofluids. Moreover, optimal SDBS concentration can result in the highest thermal conductivity of the nanofluids[1].

Although the influence of surfactant on the thermophysical properties of nanofluids is not negligible, it is moderate and predictable for the application in single-phase heat transfer apparatus providing the measured properties were used. Recently, more attention have been paid to the boiling heat transfer of nanofluids. This is where surfactant can play a key role; boiling mechanisms are highly dependent on the surface wetting and surfactant could change the surface tension of fluids and hence the contact angle. Therefore it is necessary to separate the effects of surfactant and nanoparticles on the surface wetting and thus boiling heat transfer. In our ongoing research, experiments were designed for the mixture of SDBS and EG-W (ethylene glycol-water mixture), and the mixture of silica

nanoparticles and EG-W, respectively; in the latter case, no surfactant were added. Only the former case will be presented in this paper.

Another focus here is the flow boiling of binary mixtures (EG-W) in a mini-tube (2.3-mm). The study of two-phase flow and flow boiling of mixtures in small and mini channels is rather rare, although the flow boiling of pure fluids in small and mini channels have been extensively investigated. The reason is probably due to the complexity and difficulty of the flow boiling phenomena of mixtures in small and mini channels. The saturation temperature of non-azeotropic mixtures depend on the mixture quality; as the more volatile component of the mixture evaporates at a faster rate, the resulting change in concentration of the phases causes an increase in the saturation temperature. This behavior could be taken advantage of in the evaporators, e.g., the temperature in the evaporator can be maintained fairly constant in spite of a decreasing pressure along the length of the evaporator [2]. Thus it is preferable to employ mixtures to compensate the non-uniformity of wall temperature due to the large two-phase pressure drop in a mini-channel. In the case of the automotive industry, the engine coolant is often a mixture of ethylene glycol and water, which is a typical non-azeotropic mixture. Thus it is necessary to conduct more investigations into the small-channel flow boiling of ethylene glycol-water mixtures.

In the present study, boiling heat transfer coefficients were determined experimentally over a range of mass flux and heat flux for the mixtures of SDBS and EG-W flowing upward in a 2.3-mm stainless steel tube. As observed in the literatures, higher concentration of SDBS dispersant (>1 wt%) could lead to reduction of the thermal conductivity and enhancement of the viscosity [3]. Therefore, a concentration of 300 ppm [1] was used in this study. Such low concentration dispersant has almost no influence on thermal conductivity and viscosity of EG-W.

2. Experimental apparatus and system validation

2.1 Two-phase loop

The heat transfer experiments were conducted in the flow loop as shown in Fig. 1. It is an open-loop system that includes a high-pressure ram-pump, a mass flowmeter, a pre-heating section, an experimental section, a condenser, and two working fluid collector. There are filters of 20-40 μ m porosity before the mass flowmeter and the back-pressure valve, respectively, to prevent the large agglomerate or other impurities entering the flow loop. A N₂ pulse damper was used to calm the fluctuation of flow. The test section consists of a tube made of stainless steel grade 304 with 2.3 mm ID, 0.4 mm thickness and 1060 mm length. Prior to its use the inner surface of the steel tube is cleaned with acetone and rinsed with deionized water to remove any dust, grease or other contaminants that could affect boiling. Ten Φ 0.3 mm T-type thermocouples (TCs) are closely attached while being electrically insulated from the outer surface of the test tube every \sim 100 mm. The test section inner wall surface temperature was determined from a radial heat conduction calculation using the measured outer surface temperature and the heat generation rate in the wall. Two submerged sheath T-type TCs measure the fluid bulk temperatures at the inlet and outlet plenums of the test section, respectively. The test section and the pre-heating section were both resistance-heated with individual, controllable DC power supplies. The power supply output regulation range is 0.2% of the voltage or current and has a power capability of up to 5 kW. The differential pressure between the inlet and outlet of the test section and the outlet pressure were also measured. The estimated uncertainty in the measurements of pressures and temperatures were \pm 1% and \pm 0.2°C, respectively. After leaving the test section, the two-phase flow was condensed into a single-phase flow and then collected to further calibrate the mass flow rate via a weighing method, the estimated uncertainty of mass flow rate was \pm 0.5%. A data acquisition system, consisting of a PC and a Hewlett-Packard multiplexor, recorded outputs from all sensors, and the data acquisition program

included all calibration equations and conversions to desired engineering units. During the test setup, the data acquisition system provided an on-screen display of sensor outputs in engineering units and graphs of representative temperatures and flow rates as a function of time to facilitate determination of steady-state conditions. When the system reached steady state at the desired parameters, the data acquisition system recorded test section sensor outputs of the wall and in-stream temperatures, power, mass flow rates, outlet pressure, and pressure drop for further data reduction.

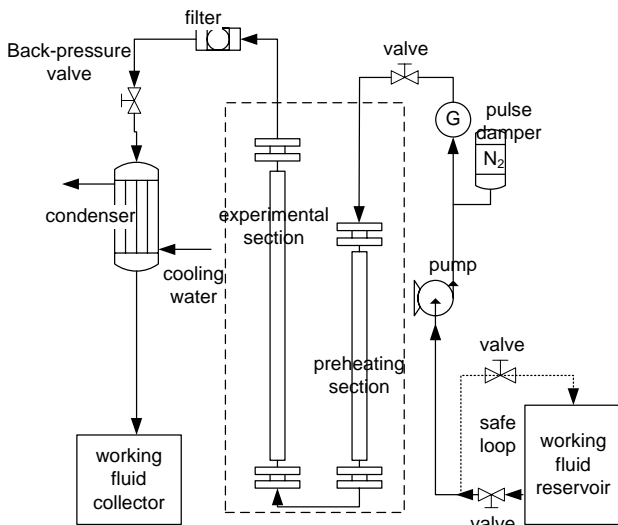


Fig. 1. Experimental facility schematic.

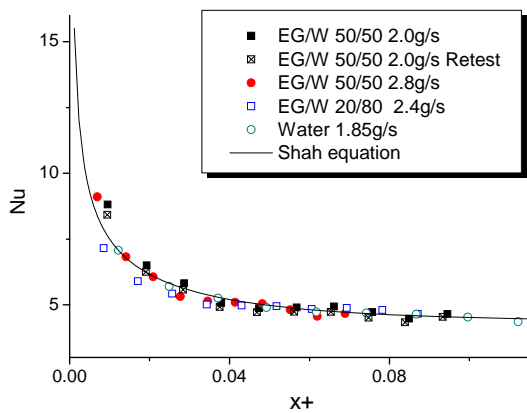


Fig. 2. The validation of single-phase heat transfer data using the Shah equation.

2.2 Heat Loss and Single-Phase Tests

Prior to performing flow boiling experiments, a series of single-phase tests were conducted within the same flow rate range. Comparison between electrical power input and water enthalpy increase during the single-phase tests proved heat loss was less than 3%. All heat flux data of the boiling tests presented in this study were therefore based on the measured electrical power input. Figure 2 shows the single-phase Nusselt numbers and the predicted values for the ethylene glycol-water mixtures and water. As shown in Figure 2, the Shah equation provides quite good predictions of the experimental data.

2.3 Boiling test procedure

The experimental procedure is as follows. After filling the loop with the test fluid, degassing is performed at 85°C for an hour. Afterwards, the flow loop components were adjusted to yield the desired inlet temperature, mass flux, as indicated in Table 1. The mass flux G was determined from measured mass flow rate, g/s. After the flow became stable, the heater power was adjusted to a level below incipient boiling. The power was then increased in small increments as the flow loop components were constantly adjusted to maintain the desired operating conditions. Once steady-state conditions prevailed, the voltage and current of the power supplies, the differential and outlet pressures, inlet and outlet temperatures, and wall temperatures were all recorded at 5 s intervals for 5 min.

Table 1

Summary of the experimental conditions.

working fluids	water	EG/W 50/50	EG/W 50/50 + 300ppm
inlet temperature oC	50		
mass flux kg/m ² s	690, 1070	640, 850, 1070, 1320	
heat flux kW/m ²	170-429	212, 248, 292, 335, 380, 433	
outlet pressure kPa	117.2-179.3	130.4-189.0	128.6-185.1
differential pressure kPa	75.7-350.5	107.0-322.3	90.0-316.0

3 Boiling Data Reduction

3.1 Physical properties evaluation

For the analysis of the data and comparison with the predictive data, all thermo-physical properties, such as density, specific heat, thermal conductivity and viscosity for both water and EG/W were taken from the ASHRAE Handbook. Thermodynamic properties, such as composition, surface tension, saturation temperature, bubble point and dew point temperatures, were obtained by combining the data from ASHRAE Handbook and Ethylene glycol/water mixture phase equilibrium diagram, as shown in Figure 3.

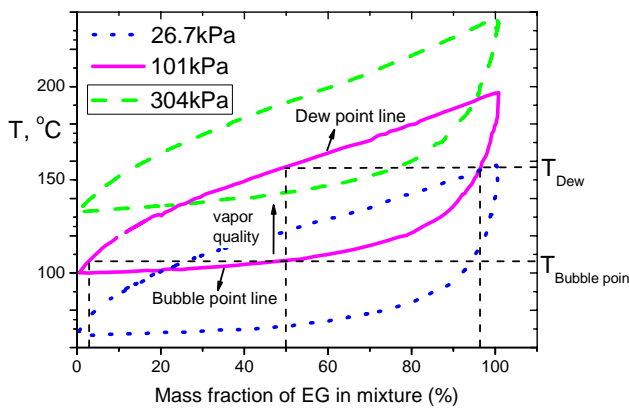


Fig. 3. Phase equilibrium diagram of ethylene glycol–water mixtures at different pressures.

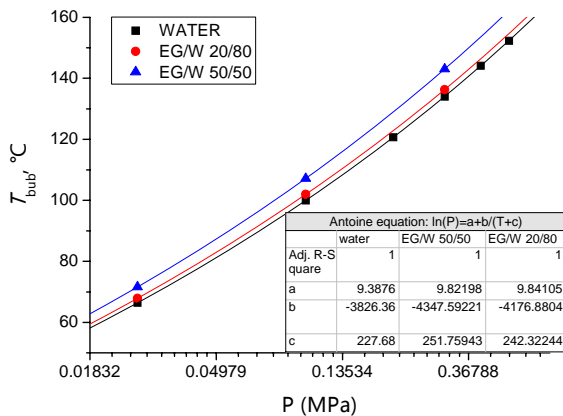


Fig. 4. Bubble point/Saturation temperature curves under different pressures.

3.2 Heat transfer characteristics

As indicated in Table 1, water was supplied into the test section in a subcooled state ($T_{f,i}=50^{\circ}\text{C}<T_{\text{sat},i}$) for all test conditions. It

is reasonable to divide the length of the tube into two regions: an upstream single-phase liquid region and a downstream saturated region. The demarcation between the two regions is the location of zero thermodynamic quality[4]. The lengths of the two regions can be evaluated from

$$L_{\text{sp}} = \frac{\dot{m}c_p (T_{\text{bub},0} - T_{f,i})}{q'' \pi D} \quad (1)$$

$$L_{\text{sat}} = L - L_{\text{sp}} \quad (2)$$

where $T_{\text{bub},0}$ is the bubble point temperature. Only for pure fluids or azeotropic mixtures, the bubble point temperature is the same as saturation temperature $T_{\text{sat},0}$. As mentioned in the introduction, the saturation temperature of two-phase non-azeotropic mixtures is dependent on the vapor quality and lies between bubble point and dew point.

To determine the $T_{\text{bub},0}$, the following approach is used. As the bubble point is a function of pressure, which is slightly decreasing along the tube in the single-phase region, we could first evaluate the $T_{\text{bub},0}$ using the indirectly measured inlet pressure, $P_{\text{out}} + \Delta P$, assuming that the pressure drop across the subcooled region is small. With the knowledge of L_{sp} , the pressure drop in the single-phase region can be calculated. Since now the local pressure of the zero thermodynamic quality location was gained, $T_{\text{bub},0}$ could be renewed. This approach is repeated until a prescribed tolerance is met. The temperature of the fluid in the single-phase region will vary linearly according to the energy balance

$$T_f = T_{f,i} + \frac{q'' \pi DL}{\dot{m}c_p}, \quad L \leq L_{\text{sp}} \quad (3)$$

where q'' is the heat flux, L means the heating length. The local heat transfer coefficient in the single-phase region can be calculated as

$$h_{\text{sp}} = \frac{q''}{T_w - T_f} \quad (4)$$

where h is the heat transfer coefficient, T_w is the wall temperature at the inside surface.

Within the saturated region, the pressure was assumed to vary linearly along the length

of the channel. Based on the local pressures, the local bubble points could be known from the knowledge of Ethylene glycol/water mixture phase diagram under different pressures. Antoine equations have been used to reproduce the bubble point data taken from the ASHRAE Handbook, as shown in Figure 4. For a binary mixture, the following equation was employed to determine the heat transfer coefficient in the saturated region as

$$h_{sat} = \frac{q''}{T_w - T_{bub}} \quad (5)$$

where the bubble point temperature rather than the saturation temperature is used according to the review of Cheng et al.[5]. Many of the open literatures do not mention which definition being used. The definition here is different from that for saturated flow boiling of pure fluids, which uses T_{sat} rather than T_{bub} in this equation. It should be noted that, during the evaporation of non-azeotropic binary mixtures, as the component concentrations in the liquid and vapor phase change along the channel, the local saturation temperature T_{sat} (i.e., T_f) becomes greater than T_{bub} (does not consider the change in compositions) as the heavy component builds up the liquid phase, as illustrated in Figure 5. The effective driving force will be $T_w - T_f$ or $T_w - T_{sat}$ but, for engineering purposes any calculation method must be based on T_{bub} . This is because the engineer might be expected to know the bulk fluid properties but the calculation of local saturation temperature is too complex for routine design calculations. Hence, the superheat, necessarily based on T_{bub} , will not be the effective value $T_w - T_{sat}$ and the heat transfer coefficient, $q''/(T_w - T_{bub})$, is underestimated, which is conservative and preferable for engineering purposes[6].

The local mass quality at a distance L from the inlet can be obtained by

$$x = \frac{Q(L/L_0) - \dot{m}(H_{sat,f} - H_i)}{\dot{m}(H_{sat,g} - H_{sat,f})} \quad (6)$$

$$= \frac{Q(L/L_0) - Q(L_{sp}/L_0)}{\dot{m}_{fg}} = \frac{Q}{\dot{m}_{fg}} \frac{L - L_{sp}}{L_0}$$

where L_0 , Q are the total channel length and power input.

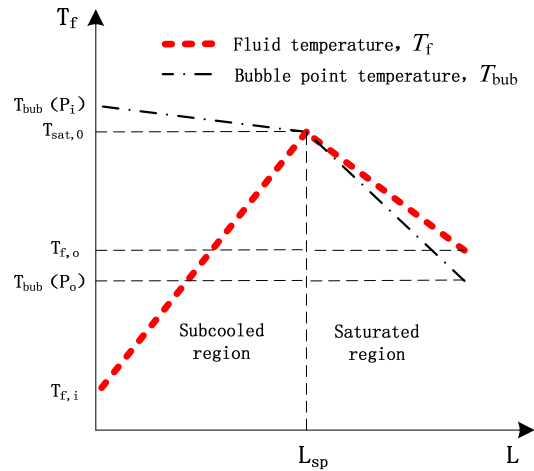


Fig. 5. Schematic representation of the fluid temperature along the mini-channel.

With the knowledge of latent vapor heat, the local quality could be calculated for water; however, the calculation will be difficult for EG/W, as the concept of the change in enthalpy of a binary fluid differs from that for a single component system since, in that case, enthalpy changes are either sensible heat changes or latent heat changes (at constant temperature). In sight of this point, some researchers utilized more complex computer codes to decide the local qualities [7, 8], which are quite too complicated for engineering purposes. For simplicity of presenting the data trend, here we define an effective vapor quality X for binary mixtures as follows

$$X = x / \left(\frac{Q}{\dot{m}_{fg}} \right) = \frac{L - L_{sp}}{L_0} \quad (7)$$

where the effect of power input and mass flow rate are not included. One should keep this in mind.

4 Results and Discussion

4.1 Flow stability of water and EG/W boiling

As one starts the tests, firstly one needs to figure out and maintain consistent and

repeatable flow boiling conditions. Note that the fluid enters into the test section at a highly subcooled state ($\Delta T_{\text{sub}} > 50^\circ\text{C}$). There is a high possibility to encounter flow instability, especially in small tubes ($D < 3\text{mm}$). In the preliminary studies, periodic and random instabilities were observed for both water and mixtures. Figure 6 shows a typical periodical oscillation of temperatures, pressures and mass flow rates. Similar condition can be found in the literature on flow boiling in microchannels, and such a flow mode is named liquid/two-phase alternating flow (LTAF) [9]. The vapor would periodically block up the mini-channel, and hence abruptly increasing temperatures and pressure drop while decreasing the mass flow rate. The changes of temperature and pressure drop are in phase, while that of temperature and mass flow rate are out of phase. Such an instability prevents one from obtaining stable heat transfer data and should be avoided in the tests. Fortunately, by further increasing the heat flux, the outlet fluid turned to be of higher vapor quality and the flow became stable enough to get the data as follows: T oscillates within 1°C (largest amplitude happened at the subcooled region, as expected), ΔP within $\pm 2\%$, and m within $\pm 1\%$. It should be noted that 50/50 EG/W was the least stable compared with 20/80 EG/W and water. A subcooled boiling region was not found in the following tests, and the boiling occurred where the bulk fluid achieved saturated state.

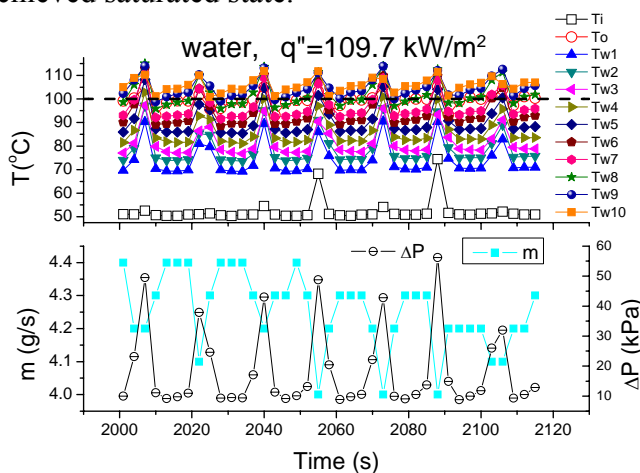


Fig. 6. Periodic instability of subcooled boiling in mini-tube.

4.2 Water data and comparison with predictive data

A set of preliminary test was conducted for pure water to set a base for comparison with mixtures and to compare with the predictive methods. Globally, the range of variation of the parameters in the tests performed is given in Table 1.

Figure 7 shows the local heat transfer coefficient along the length of the tube with increasing vapor mass quality. For both mass fluxes, the heat transfer coefficient initially increased then, monotonically decreased. Previous studies conjectured that the possible reason for this decreasing heat transfer coefficient is local dryout [10]. The quality where the heat transfer coefficient started to decrease was defined as the critical quality, x_{crit} , which is approximately 0.1 in this study. Another insight could be gained from the boiling curves at the outlet three locations, as shown in Figure 8. The independence of heat transfer coefficient on heat flux at T_{w9} and T_{w10} for $690 \text{ kg/m}^2\text{s}$ suggests that nucleate boiling might not be the dominant heat transfer mechanism at these regions. While the boiling curve at T_{w8} clearly exhibits nucleate heat transfer mechanism. After that location, higher vapor quality seems to deteriorate the heat transfer.

To further understand the data, the experimental results obtained are compared to predictions from several correlations from the literature. Of the many predictive correlations for boiling heat transfer, the one by Cooper [11] is widely used for predicting nucleate pool boiling heat transfer coefficients. The Chen correlation and the Steiner-Taborek asymptotic model, considering superposition of nucleate boiling and forced convection component, were also included to predict the present data. Among the three correlations considered, Cooper's nucleate pool boiling correlation best predicts the experimental results from the present work. The Cooper correlation correctly predicts the trend of heat transfer coefficient with heat flux and local reduced pressure. Except for three points, all the data are predicted within $\pm 30\%$. The mean absolute

percentage error (MAPE) is 12.9%, as seen in Figure 9. The other two correlations highly overpredict the experimental results and therefore are not presented here.

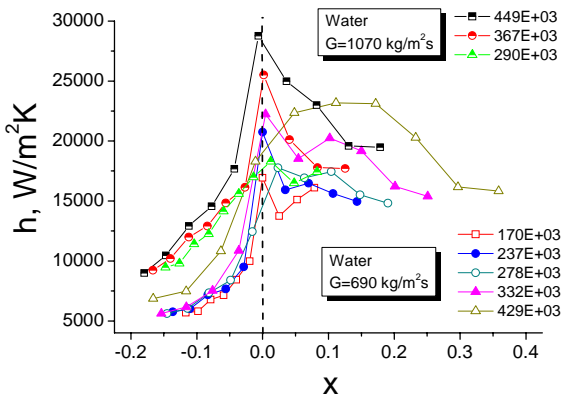


Fig. 7. Heat transfer coefficient for water as a function of heat flux at $G = 690\text{kg/m}^2\text{s}$ and $1070\text{kg/m}^2\text{s}$.

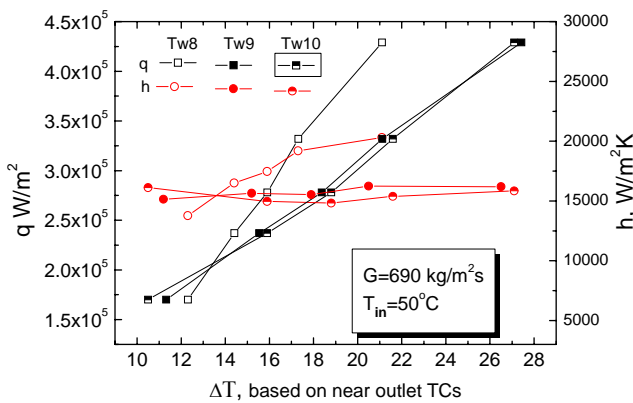


Fig. 8. Heat flux and heat transfer coefficient as a function of wall superheat in water experiments: boiling regions.

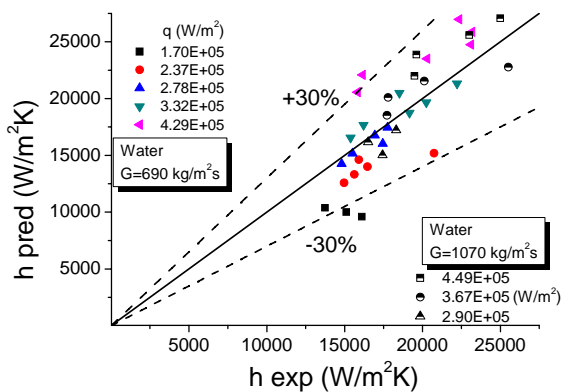
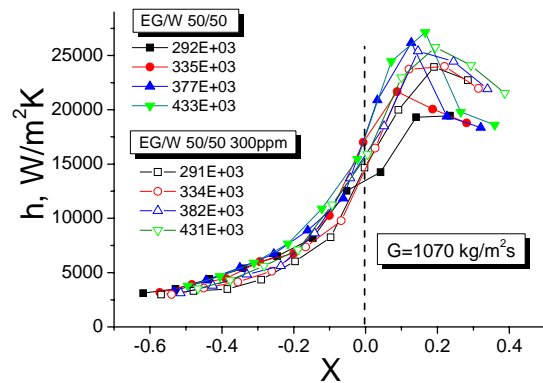


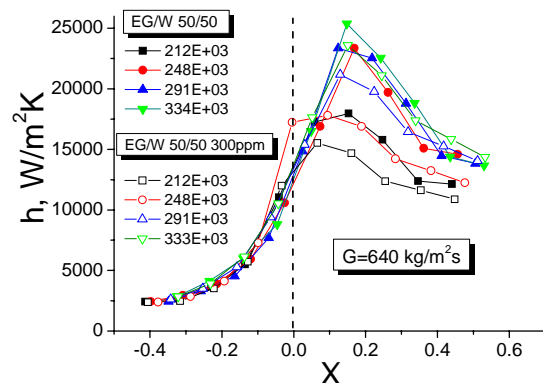
Fig. 9. Boiling heat transfer data compared with Cooper correlation.

4.3 EG/W data and comparison with SDBS solutions

The results of EG/W and 300 ppm SDBS solutions for 1070 and 640 $\text{kg/m}^2\text{s}$ are presented in Figure 10. It should be noted that the effective quality, X , only serves as a tool to present the trend of HTC. The true quality should be more scattered than in Figure 10 (due to range of heat input, Q) and relatively small for 1070 $\text{kg/m}^2\text{s}$ compared to that of lower mass flux ($x = X(Q/mi_{fg})$).



(a) higher mass flux



(b) lower mass flux

Fig. 10. Heat transfer coefficient of EG/W mixture and 300ppm SDBS solution for different heat fluxes.

For 1070 $\text{kg/m}^2\text{s}$, after a sharp increase at low qualities, the local two-phase heat transfer coefficient of EG/W and 300 ppm SDBS solutions both drops and converges to two different groups. The maximum value should be obtained in slug flow when the liquid layer

thickness reaches its minimum value. The heat transfer deterioration occurs when the slug flow is disrupted to become slug-annular or churn flow. There will be intermittent dryout in the semi-annular and churn flow, and the liquid film thickness will increase in wavy conditions. While the EG/W exhibits a sharp decrease of HTC after the apex, the SDBS solutions maintain a relatively high HTC. The addition of trace SDBS remarkably enhanced the boiling heat transfer after the critical effective quality. The surfactant SDBS promotes the nucleation and evaporation, and therefore enhances the heat transfer. Evidence of more vigorous vaporization could be found from the difference between the outlet fluid temperature and outlet bubble point temperature. As introduced in section 3.2 and Figure 5, the higher the vapor quality, the higher the fluid temperature grows than the bubble point responding to the original binary mixture. Figure 11 shows that the temperature differences are about 3 °C for SDBS solutions and 1.5 °C for EG/W.

For 640 kg/m²s, the trend is somewhat different. Generally, the boiling heat transfer coefficient of 300 ppm SDBS solutions is lower than that of EG/W. The greatest reduction corresponds to the heat flux of 248 kW/m², where the vaporization process should be the most vigorous according to Fig. 11. Qualities higher than a critical value would lead to severe deterioration of HTC due to intermittent dryout. The more vapor in the core flow, the more deterioration. The temperature gap between the fluid temperature and bubble point is about 7 °C for SDBS solutions and 3.5 °C for EG/W on average, suggesting much higher true outlet quality than that of the EG/W mixture and also the condition of 1070 kg/m²s.

In summary of these mini-channel flow boiling tests, such a phenomenon is general for both the EG/W mixtures, SDBS solutions and water: the local heat transfer coefficient increases with vapor quality up to a critical value of the vapor quality beyond which, its deterioration occurs. Deterioration of the heat transfer coefficient is believed to be caused by the intermittent dryout, which refers to an

unstable breakdown of the liquid film in contact with the wall. In the literature, it is found that the critical vapor quality decrease with an increase of the mass velocity. This trend is clearly proved in the water test (Fig. 7): the heat transfer coefficient for higher mass flux decreases immediately after the zero quality, while that for lower mass flux will experience firstly an increase and later a decrease. To validate this trend in EG/W mixtures, experiments under various mass fluxes were conducted. As shown in Fig. 12, the critical effective qualities, X , are all close to 0.1. However, the fact that the real quality of EG/W mixtures, x , is inversely proportional to the mass flow rate ($x=X(Q/mi_{fg})$), indicates that the critical real quality is lower for higher mass fluxes.

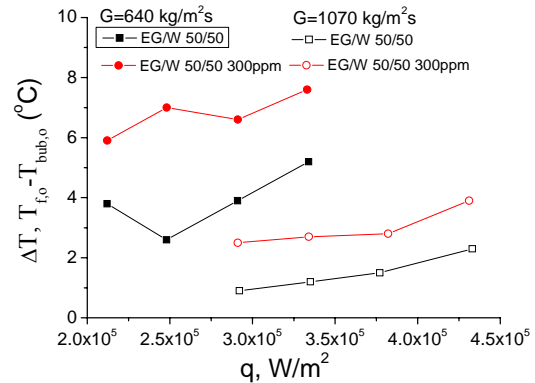


Fig. 11. Difference between outlet fluid temperature and bubble point temperature.

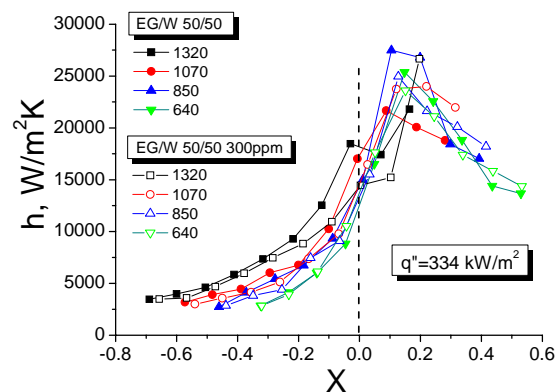


Fig. 12. Heat transfer coefficient of EG/W mixture and 300ppm SDBS solution for different mass fluxes.

5. Conclusions

The upward flow boiling heat transfer of water and ethylene glycol/water mixtures in a vertical mini-tube was experimentally determined. Effects of trace (300 ppm) surfactant, SDBS, on the boiling heat transfer were discussed for various mass fluxes and heat fluxes. The main findings are as follows:

(1) Periodic flow instability, or the liquid/two-phase alternating flow was encountered in the subcooled flow boiling of water, oscillations of pressure drop and wall temperature are nearly in phase while that of mass flux and wall temperature are nearly out of phase. Stable results were obtained only in the saturated boiling region.

(2) Experiments of water and ethylene glycol/water mixtures were conducted in similar ranges. Experimental results of water were well predicted within $\pm 30\%$ by the Cooper correlation, which is developed for pool nucleate boiling. The trend of the heat transfer coefficient with local quality were similar for all the working fluids: there was an apex.

(3) In the lower mass flux region, the addition of surfactant causes general deterioration of the boiling heat transfer coefficient, while in the higher mass flux region the surfactant enhances the heat transfer after the critical effective quality. After a critical quality, higher quality will deteriorate the heat transfer due to intermittent dryout, therefore adding surfactant to generate more vapor may have a negative effect on the heat transfer of flow boiling in a mini-tube, which is in contrast to the experience of enhancing nucleate pool boiling heat transfer with trace surfactant. However, as the real quality is unknown due to the complexity of obtaining vapor latent heat, consistent conclusion on the heat transfer characteristics of EG/W mixtures and SDBS solutions cannot be drawn yet.

Acknowledgements

Z. Feng and W. Li greatly appreciate financial support from the National Natural Science Foundation of China. Z. Wu and B. Sunden gratefully acknowledge the financial

support from the Swedish Energy Agency and the Swedish Research Council.

References

- [1]. Wang, X., D. Zhu and S. Yang, Investigation of pH and SDBS on enhancement of thermal conductivity in nanofluids. *Chemical Physics Letters*, 2009. 470(1-3): p. 107-111.
- [2]. Raykoff, T., Bubble growth rate and heat transfer suppression in the flow boiling of binary mixtures. 1996.
- [3]. LotfizadehDehkordi, B., et al., Investigation of viscosity and thermal conductivity of alumina nanofluids with addition of SDBS. *Heat and Mass Transfer*, 2013. 49(8): p. 1109-1115.
- [4]. Lee, P. and S.V. Garimella, Saturated flow boiling heat transfer and pressure drop in silicon microchannel arrays. *International Journal of Heat and Mass Transfer*, 2008. 51(3-4): p. 789-806.
- [5]. Cheng, L. and D. Mewes, Review of two-phase flow and flow boiling of mixtures in small and mini channels. *International Journal of Multiphase Flow*, 2006. 32(2): p. 183-207.
- [6]. SARDESAI, R.G., R.A.W. SHOCK and D. BUTTERWORTH, *Heat and Mass Transfer in Multicomponent Condensation and Boiling*. *Heat Transfer Engineering*, 1982. 3(3-4): p. 104-114.
- [7]. Yu, W., et al., Small-Channel Flow Boiling of One-Component Fluids and an Ethylene Glycol/Water Mixture*. *Experimental Heat Transfer*, 2005. 18(4): p. 243-257.
- [8]. Yu, W., D.M. France and J.L. Routbort, Pressure drop, heat transfer, critical heat flux, and flow stability of two-phase flow boiling of water and ethylene glycol/water mixtures-final report for project. 2011, Argonne National Laboratory (ANL).
- [9]. Wu, H.Y. and P. Cheng, Boiling instability in parallel silicon microchannels at different heat flux. *International Journal of Heat and Mass Transfer*, 2004. 47(17-18): p. 3631-3641.
- [10]. Thome, J.R., V. Dupont and A.M. Jacobi, Heat transfer model for evaporation in microchannels. Part I: presentation of the model. *International Journal of Heat and Mass Transfer*, 2004. 47(14): p. 3375-3385.
- [11]. Cooper, M.G. Saturation nucleate pool boiling: a simple correlation. in 1st UK National Conference on Heat Transfer. 1984.